

## Supporting information

### **SERS and fluorescence dual-channel microfluidic droplet platform for exploring telomerase activity at single-cell level**

Guohua Qi<sup>b</sup>, Xuan Yi<sup>a</sup>, Minmin Wang<sup>c</sup>, Dan Sun<sup>a,\*</sup>, Hongyan Zhu<sup>a,\*</sup>

- a. School of Pharmacy, Nantong University, Nantong, Jiangsu 226001, China
- b. State Key Laboratory of Electroanalytical Chemistry, Changchun Institute of Applied Chemistry, Chinese Academy of Sciences, Changchun 130022, Jilin, P. R. China
- c. School of Chemistry and Chemical Engineering, Nantong University, Nantong, Jiangsu, 226019, China

\* Corresponding author.

E-mail addresses: dsun1203@ntu.edu.cn (D. Sun) amyntu@126.com (H. Y. Zhu)

## 1. Materials and methods

### 1.1 Materials and instruments

Gold(III) chloride trihydrate, trisodium citrate (98%), alkaline phosphatase (ALP), bovine serum albumin (BSA), thrombin, trypsin, epigallocatechin gallate (EGCG) were obtained from Aladdin Industrial Corporation (Shanghai, China). The certified fetal bovine serum was purchased from VivaCell, Shanghai, China. Deoxynucleotide triphosphates (dNTPs) were purchased from the Sigma-Aldrich (USA). SU-8 2025 was purchased from Microchem. Sylgard 184 poly(dimethylsiloxane) (PDMS) and crosslinker were obtained from Dow Corning, Midland, MI. Fluorinert HFE-7500 fluorocarbon oil was purchased from 3M, St. Paul, MN. PFPE-PEG block-copolymer surfactant was bought from Ranbiotech.

The morphologies of the AuNPs were characterized by the transmission electron microscope (TEM, Hitachi 600). The UV-vis absorption spectra of AuNPs, DNA and nanoprobe were obtained with a Lambda 750 spectrophotometer (Perkin-Elmer). The zeta-potential of AuNPs and nanoprobe were characterized by the dynamic light scattering (90 plus Zeta, BROOKHAVEN). The confocal fluorescence imaging was performed using a laser scanning confocal microscopy (TCS SP8, Leica, Germany). The SERS measurement by a confocal Raman system (Thermo Fisher Scientific Co., Ltd.) with a 633 nm laser as an excitation source and an integration time of 15 s.

### 1.2 Preparation of the nanoprobe

The AuNPs used in this work were prepared according to the classic citrate reduction reaction. The primer sequences and Cy5 labeled DNA strand (Table S1) were dissolved in PBS, then the mixed solution was heated to 95 °C for 10 min, naturally cooled at room temperature slowly. Then, 50 μL of primer sequences ( $1.0 \times 10^{-6}$  M) and 50 μL of Cy5 labeled DNA strand ( $1.0 \times 10^{-6}$  M) were sequentially added to 1 mL of the prepared colloid gold (1.4 nM). The mixture was placed at 37 °C and gently shaken for 14 h. Finally, the mixed solution was centrifuged (10000 rpm, 20 min) for two times. After centrifugation, the sediment was re-dispersed in PBS solution (0.2 M NaCl) to obtain a SERS-fluorescence dual-signal switchable nanoprobe.

### 1.3 Droplet formation, cell culture and encapsulation

For water-in-oil droplets formation, Fluorinert HFE-7500 fluorocarbon oil (2% w/w PFPE-PEG block-copolymer surfactant) and the cell suspension are used as the oil phase and water phase, and the flow rates are 820  $\mu\text{L}/\text{h}$  and 40  $\mu\text{L}/\text{h}$ , respectively. The water phase is dispersed in immiscible oil phase to form droplets encapsulating individual cells.

The normal liver (LO2), liver cancer (HepG2) and breast cancer (MCF-7) cells lines were purchased from Shanghai ATCC cell bank. These cells were cultured in Dulbecco's Modified Eagle Medium (DMEM, Gibcos) containing 10% fetal bovine serum (FBS) at 37 °C, 5%  $\text{CO}_2$ . The nanoprobe were added to the petri dish and co-cultured with cells for 3.5 h, the cells were washed using PBS (3 times) to clear away excess nanoprobe. Then trypsin (wt 0.25%) was used for digesting the treated cells (2 min) to acquire the cell suspension. Detailed experimental steps of the single-cell encapsulation in droplets are shown in works that we have reported previously.<sup>1</sup>

### 1.4 Detection of telomerase activity in PBS

Condition optimization of evaluation of telomerase activity was first carried out. As shown in Fig. S2, 80 min and 35 °C were chosen as the optimum reaction time and temperature value, respectively. Then, RNase inhibitor, 8  $\mu\text{L}$  of telomerase ( $10^{-10}$  IU) and 8  $\mu\text{L}$  of dNTPs (10 mM) were added to 400  $\mu\text{L}$  of nanoprobe and the reaction was allowed to stand for 80 min. Then the resulting solution was used for fluorescence and SERS measurement.

To order to obtain a standard curve for detecting telomerase activity in droplets, nanoprobe and different telomerase activity ( $1.0 \times 10^{-13}$  IU to  $1.0 \times 10^{-8}$  IU) were co-encapsulated into dispersed droplets. We used glass vials to collect generated droplets for 25 min. Then, the collected drops were re-injected into a microfluidic readout chip. SERS detection at target location within droplets was executed with a confocal Raman spectrometer. The laser wavelength and accumulation time used in this experiment is 633 nm and 15 s, respectively.

### 1.5 Fluorescence imaging analysis of telomerase activity

The cell endocytosed with nanoprobe is used as an aqueous phase to encapsulate

into the droplet. The collected droplets were incubated for 4 h (at room temperature). Then, these droplets were used for fluorescence imaging with an inverted scanning laser confocal microscope. A 10×objective was used to collect the cellular images in droplets. The excitation wavelength for probe molecule (Cy5) was 650 nm.

### 1.6 SERS detection of telomerase in single cells

The prepared droplets containing a single cell endocytosed with nanoprobe were introduced to microfluidic readout chip. Then, this chip was placed on the stage of a confocal Raman system (Thermo Fisher Scientific Co., Ltd.) to acquire the SERS spectra of droplets loaded with a single cell. All the SERS spectra were collected by 633 nm with an integration time of 25 s and one accumulation.

## 2. The feasibility of the nanoprobe for detecting telomerase in droplets

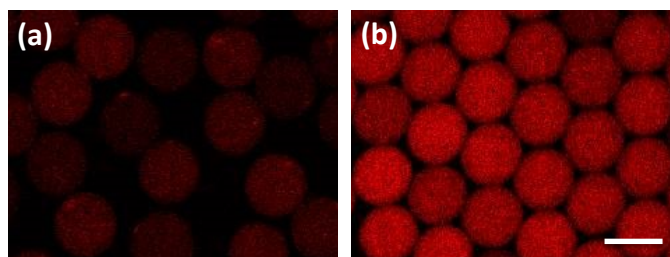


Fig. S1. Fluorescence images of the nanoprobe without (a) or with (b) telomerase ( $1.0 \times 10^{-8}$  IU) in the droplet. Scale bar represents 90  $\mu\text{m}$ .

## 3. Optimization of the reaction conditions between telomerase and nanoprobe

Condition optimization for detecting telomerase activity was carried out. The incubation time for SERS intensity of nanoprobe at  $1361 \text{ cm}^{-1}$  in the presence of telomerase ( $1.0 \times 10^{-10}$  IU) was assessed in Fig. S2a. It is noted that SERS intensity at  $1361 \text{ cm}^{-1}$  is sharply decreased within the first 80 min. When the reaction time is 80 min, the SERS intensity of  $1361 \text{ cm}^{-1}$  reaches the minimum value, and then the value remains almost unchanged with time (Fig. S2b). Thus, 80 min is chosen as the optimum incubation time. Furthermore, the SERS intensity of nanoprobe was investigated under different temperature. The influence of temperature values ranging from 20 to  $45^\circ\text{C}$  on the SERS signal intensity produced by  $1.0 \times 10^{-10}$  IU telomerase is shown in Fig. S2c and the SERS intensity at  $1361 \text{ cm}^{-1}$  reached a minimum at  $35^\circ\text{C}$ . Therefore, we selected  $35^\circ\text{C}$  as the optimum temperature.

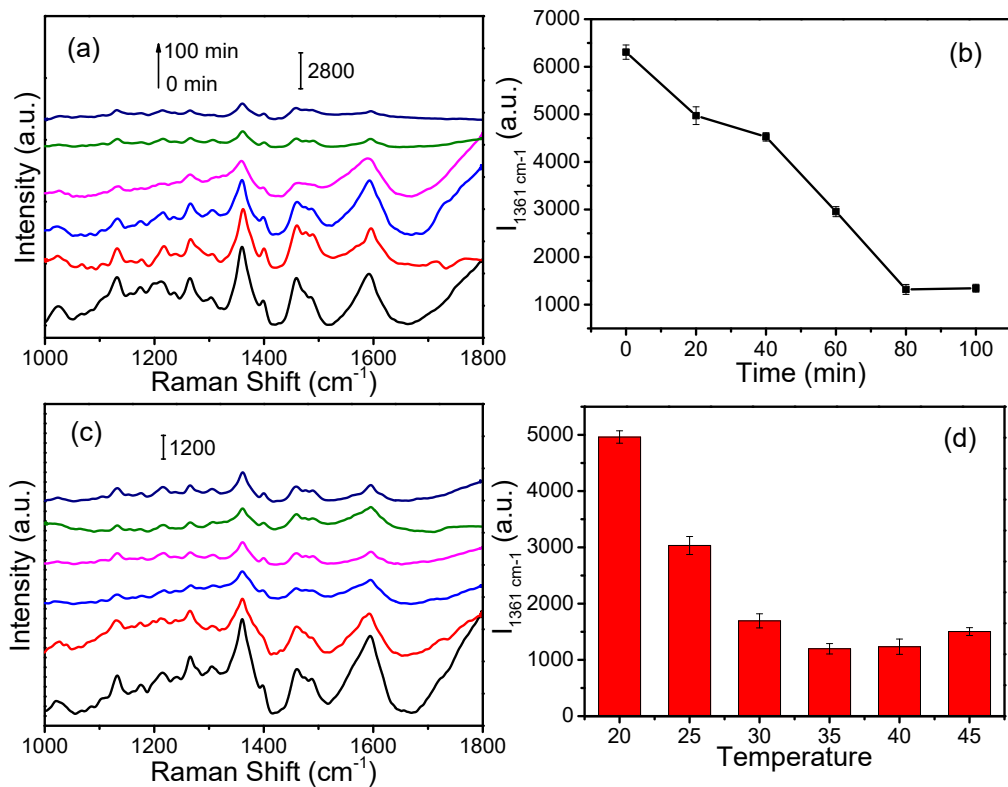


Fig. S2. (a) SERS spectra of nanoprobe at different reaction time (from bottom to top: 0 20, 40, 60, 80 and 100 min, respectively) (b) A plot of the SERS intensity of nanoprobe at  $1361 \text{ cm}^{-1}$  along with reaction time. (c) SERS spectra of nanoprobe at different temperature (from bottom to top are  $20, 25, 30, 35, 40, 45^\circ\text{C}$ ), while the reaction time kept at 80 min. (d) Plot of SERS intensity at  $1361 \text{ cm}^{-1}$  with the temperature.

#### 4. Evaluation of selectivity for detecting telomerase

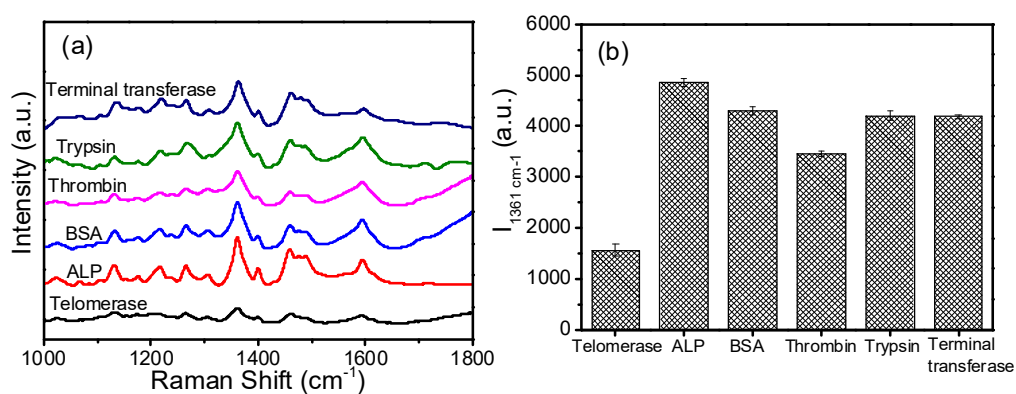


Fig. S3. (a) SERS spectra and (b) corresponding histogram studies of selectivity of this method with telomerase ( $10^{-10}$  IU) and other enzymes ( $10^{-8}$  IU).

## 5. Evaluation of stability for detecting telomerase

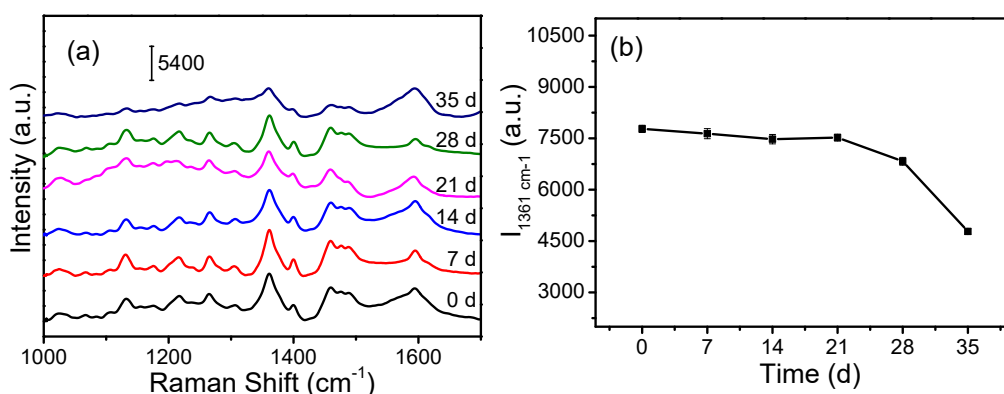


Fig. S4. (a) SERS spectra of nanoprobes were placed for different days (from bottom to top: 0, 7, 14, 21, 28, 35 d). (b) The stability evaluation of the nanoprobes.

## 6. Detection of telomerase activity by fluorescence

We have also collected fluorescence spectra with different telomerase activity and the corresponding results are shown in Fig. S5. With the increase of telomerase activity, the fluorescence intensity of Cy5 increased gradually. The linear correlation coefficient in the  $10^{-12}$ - $10^{-8}$  IU interval is 0.921, which is smaller than the result of SERS spectra. This indicates that the SERS strategy of this method has a better linear correlation for detecting telomerase than fluorescence. In addition, the lowest detection activity for telomerase obtained by the SERS strategy ( $1.0 \times 10^{-13}$  IU) is also lower than that of fluorescence ( $1.0 \times 10^{-12}$  IU), demonstrating that SERS is more sensitive than fluorescence in this method.

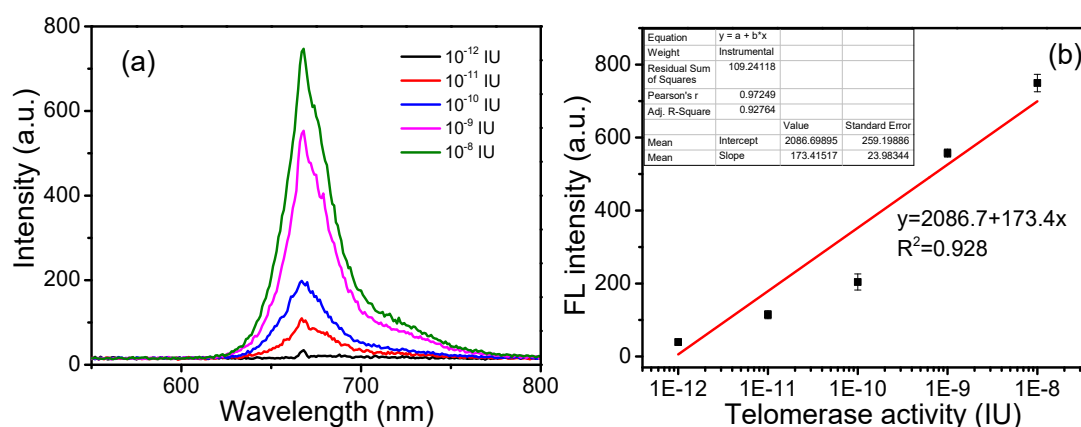


Fig. S5. (a) Fluorescence spectra of the nanoprobes in the appearance of different telomerase activity (from bottom to top  $1.0 \times 10^{-12}$ ,  $1.0 \times 10^{-11}$ ,  $1.0 \times 10^{-10}$ ,  $1.0 \times 10^{-9}$ ,  $1.0 \times 10^{-8}$  IU). (b) A plot of the fluorescence intensity of Cy5 at 668 nm along with the telomerase activity.

## 7. Optimization of endocytosis time of nanoprobes

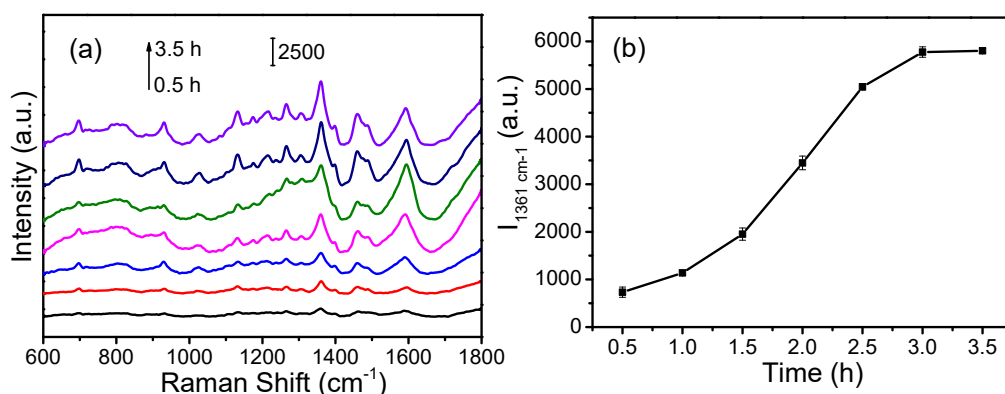


Fig. S6. (a) SERS spectra of HepG2 cells incubated with 0.35 nM nanoprobe for different time (from bottom to top: 0.5, 1.0, 1.5, 2.0, 2.5, 3.0 and 3.5 h). (b) A plot of the SERS intensity of Cy5 at 1361 cm<sup>-1</sup> along with incubation time.

## 8. The number of nanoparticles swallowed by different kind of cell

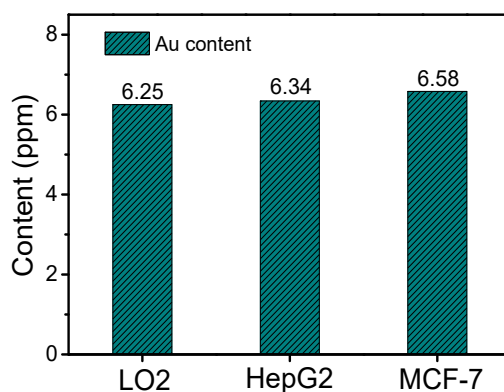


Fig. S7. The nanoprobe uptaken by three cell lines (LO2, HepG2 and MCF-7 cells) for 6 h detected by ICP-MS.

## 9. The efficiency of droplet encapsulating single cell

The efficiency of produced droplets encapsulating single cells was evaluated in by the Poisson distribution (Fig. S8). The Poisson distribution of cells encapsulated into droplets is given as following:

$$f(\lambda; n) = (\lambda^n e^{-\lambda}) / n!$$

where  $n$  is the number of cells in the droplets and  $\lambda$  is the average value of cells encapsulated into per droplet. We have calculated the distributions under the different densities of cells into every droplets. The values of  $\lambda$  were 0.2, 0.3, and 0.4 respectively, which are typical values of interest for single cell experiments. It can

ensure that very few droplets containing multiple cells. In our work, the value of  $\lambda$  used is about 0.3 which is in good agreement with those results calculated from Poisson statistics (Fig. S8) under the density of cells about  $3.1 \times 10^6$  cells/mL. Therefore, we have obtained the probability of single cells encapsulated into one droplet was about  $\sim 20\%$  while ensuring that fewer than 7% have two or more cells. Although the number of single-cell-bearing droplets is rather low, it could not influence the detection of single cells in this work, because the high production and screening rate can be achieved with microfluidic devices to obtain the single cells encapsulated into one droplet.

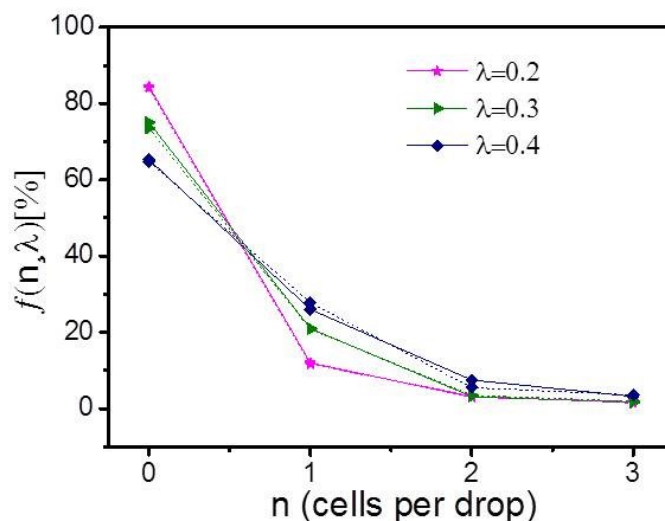


Fig. S8. The probability of a droplet encapsulating a single cell.  $n$  is the number of cells in the drops and  $\lambda$  is the average number of cells per droplet. Dashed and solid lines show the predicted values from Poisson statistics and experimental results.

## 10. DNA sequences information

Table S1. Oligonucleotide sequences used in our experiments

| Oligonucleotides name | Sequences                                   |
|-----------------------|---|
| TS                    | 5'-HS-CCCTAACCTAACCTAAAATCCGTCGAGCAGAGTT-3' |
| Cy5-DNA               | 5'-ATGTGAATTCGGATTTTAGGGTTAACACAT-(Cy5)-3'  |



## 11. Band assignments

Table S2. The assignments of SERS bands of Cy5.

| Raman Shift (cm <sup>-1</sup> ) | Assignment                           |
|---------------------------------|--------------------------------------|
| 1032                            | alkane chain linker                  |
| 1133                            | C–H in-plane bending                 |
| 1216                            | C–N stretching                       |
| 1265                            | C–N–C symmetric stretching           |
| 1361                            | CH <sub>2</sub> in-plane deformation |
| 1459                            | C=C, ring-stretching                 |
| 1595                            | C=N stretching                       |

### References

- 1 D. Sun, F. H. Cao, L. L. Cong, W. Q. Xu, Q. D. Chen, W. Shi and S. P. Xu, *Lab Chip*, 2019, **19**, 335-342.